REFERENCES

[1] Huang J, Encinar JA. *Reflectarray Antenna*. John Wiley & Sons, Inc. Hoboken, NJ; 2005.

[2] Hosseini A, Capolino F, De Flaviis F. Gain enhancement of a V-band antenna using a fabry-perot cavity with a self-sustained all-metal cap with FSS. *IEEE Tran Antennas Propag*. 2015;63(3):909–921.

[3] Yu A, Yang F, Elsherbeni A, Huang J. Transmitarray antennas: an overview. In: USNC/URSI Radio Science Meeting, Spokane, Washington, USA; 2011.

[4] Padilla Munoz-Acevedo P, Sierra-Castaner AM, Sierra-Perez M. Electronically reconfigurable transmitarray at Ku band for microwave applications. *IEEE Trans Antennas Propag*. 2010;58(8):2571–2579.

[5] Ryan CGM, Chaharmir M, Shaker RJ, Bray JR, Antar YMM, Ittipiboon A. A wideband transmitarray using dual-resonant double square rings. *IEEE Trans Antennas Propag*. 2010;58(5):1486–1493.

[6] Jazi MN, Chaharmir M, Shaker RJ, Sebak AR. Broadband transmitarray antenna design using polarization-insensitive frequency selective surfaces. *IEEE Trans Antennas Propag*. 2016;64(1):99–108.

[7] Rahmati B, Hassani HR. High-efficient wideband slot transmitarray antenna. *IEEE Trans Antennas Propag*. 2015;63(11):5149–5155.

[8] Abdelrahman A, Nayeri HP, Elsherbeni AZ, Yang F. Bandwidth improvement methods of transmitarray antennas. *IEEE Trans Antennas Propag*. 2015;63(7):2946–2954.

[9] Cheng Q, Ma HF, Cui TJ. Broadband planar Luneburg lens based on complementary metamaterials. *Appl Phys Lett*. 2009;95(18):181901.

[10] Clemente Dussopt A, Sauleau L, Potier RP, Pouliguen P. Wideband 400-element electronically reconfigurable transmitarray in X band. *IEEE Trans Antennas Propag*. 2013;61(10):5017–5027.

[11] Rahmati B, Hassani HR. Low-profile slot transmitarray antenna. *IEEE Trans Antennas Propag*. 2015;63(1):174–181.

[12] Abdelrahman AH, Elsherbeni AZ, Yang F. Transmission phase limit of multilayer frequency-selective surfaces for transmitarray designs. *IEEE Trans Antennas Propag*. 2014;62(2):690–697.

[13] Luo J, Yang F, Xu S. E-shaped element design for linearly polarized transmitarray antennas. In Antennas and Propagation (ISAP), 2014 International Symposium on 2014:269–270.

[14] Datthanasombat S, Prata A, Jr,Arnaro L, Harrell J, Spitz S, Perret J. Layered lens antennas. In Antennas and Propagation Society International Symposium, 2001. IEEE; 2001:777–780.

[15] Cheng CC, Abbaspour-Tamijani A. Study of 2-bit antenna-filter-antenna elements for reconfigurable millimeter-wave lens arrays. *IEEE Trans Microw Theory*. 2006;54(12):4498–4506.

How to cite this article: Luo J, Yang F, Xu S, Li M, Gu S. A high gain broadband transmitarray antenna using dual-resonant E-shaped element. *Microw Opt Technol Lett*. 2018;60:1531–1536. https://doi.org/10.1002/mop.31197

Received: 11 November 2017

DOI: 10.1002/mop.31196

VHF suspended plate transmitter antenna design for DVB-T and DAB-T

Abdul Ali[1] | Mehmet Ciydem[2] | Ayhan Altintas[3] | Sencer Koc[4]

[1] Department of Electronics Engineering, University of Roma Tor Vergata, Rome, Italy

[2] Engitek Ltd., Ankara, Turkey

[3] Electrical and Electronics Engineering Department, Bilkent University, Ankara, Turkey

[4] Electrical and Electronics Engineering Department, Middle East Technical University, Ankara, Turkey

Correspondence
Abdul Ali, Department of Electronics Engineering, University of Roma Tor Vergata, Rome, Italy.
Email: abdul.ali@uniroma2.it

Abstract

This paper presents the design of stacked suspended plate transmitter antenna for digital video and audio broadcasting. Contrary to conventional dipole structures, we have designed the antenna in VHF band (174–254 MHz) with two plates for wideband matching and design flexibility. Radiating primary plate has been excited by novel wideband modified inverted L-type probe. Parasitic secondary plate, and vertical wall between primary plate, and ground plane have been used for further matching and beamwidth adjustment. A bandwidth of 42% and gain of 8.5 dBi is obtained at center frequency. Together with equivalent lumped element circuit model of designed antenna and experimental results for S_{11}, gain, and radiation pattern are presented. To the best of authors knowledge this is the first stacked suspended plate antenna achieving a record bandwidth of 42% in VHF band.

KEYWORDS

DAB-T, DVB-T, equivalent circuit model, inverted L-type probe, SSPA

1 | INTRODUCTION

PLANAR antennas such as microstrip patch/plate antennas have attracted many researchers due to their low profile, light

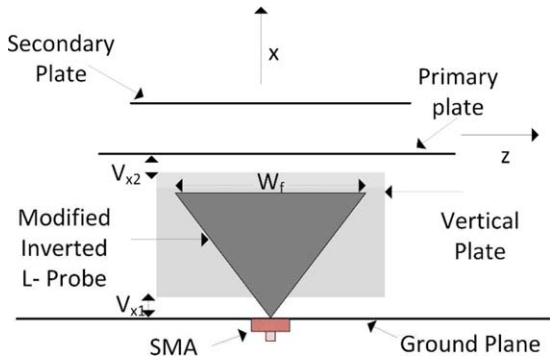

FIGURE 1 Geometry of the SSPA, front view showing feeding mechanism, ground plane, primary plate, secondary plate, and vertical plate [Color figure can be viewed at wileyonlinelibrary.com]

weight, easy fabrication, low cost, conformability, and versatility.[1,2] Up to date numerous microstrip antennas have been designed which provides interesting characteristics.[1-23] However, most of them have some major disadvantages, which makes them no-suitable for practical applications, for instance small bandwidth, low gain, and poor radiation performance.[1] Many techniques have been used to improve the impedance bandwidth, gain, directivity, and radiation performance of microstrip patch/plate antennas such as use of metamaterials, electromagnetic bandgap structures, varying shapes of patches, adding parasitic patches and shorting pins, use of low permittivity substrates and different feeding mechanism.[3-23]

In Ref. [1], impedance bandwidth is broadened by means of using a thick dielectric substrate, but it also degrades the radiation efficiency due to generation of surface waves.[2] Low dielectric substrate helps in suppressing surface waves. The bandwidth can also be increased by changing the shape of the antennas for instance, use of *E* shaped plates, slotted antennas and combination of slotted and *E* shaped plate antennas. *E* shaped antenna with corrugated wings is reported in Ref. [3] while for the combination of two different shapes, a half *U* slot and half *E* shaped plate antenna design is discussed in Ref. [4]. Probe feeding mechanism is utilized to enhance the bandwidth of stacked patch antennas.[5–10] Despite of giving good impedance bandwidth by the antennas reported in Refs. [1,3–7], they give poor radiation performance in the sense of cross polarization levels. Single and multiple port feeding structures are also used to make the bandwidth wider while maintaining acceptable radiation efficiency.[11–18]

Works in Refs. [11,12] address the radiation performance of single port center fed patch antennas, while the antenna discussed in Ref. [13] uses shorting strips and slots for the same purpose, but again the impedance bandwidth is affected. Four port capacitive probe feeding is applied in Ref. [14] to get broad bandwidth and radiation performance in VHF band, but the coupling between input ports degrades the return loss. The coupling is reduced by using multiple shorting pins. In Ref. [15], single-feed, circularly polarized (CP) stacked plate antenna is used for UHF RFID reader applications. Dual L-shaped strips or single modified L-shaped strip that employs electromagnetic coupling to cancel the excessive inductance introduce from probe feed strip are discussed in Refs. [16–18].

Furthermore, in Refs. [19–21], the impedance bandwidth is improved by means of non-planar radiating plate and making the middle portion of probe feed plate antenna concaved to form a V like structure to get a bandwidth of about 60%. However, the method suffers from bad radiation pattern performance, which is further improved in Ref. [21] using tapered down feeding strip mechanism. It gives dipole like radiation pattern. Indeed, a single port stacked suspended plate antenna is required to provide wideband matching and enhanced radiation performance, simultaneously.

In this paper, the design of a stacked suspended plate antenna (SSPA) for digital video and audio broadcast application is proposed in the VHF band. The proposed SSPA consists of a novel wideband modified inverted L-type probe feeding mechanism to excite the primary radiating plate in a capacitively coupled manner. Wideband matching is achieved through determination of the suitable positions of suspended plates. A vertical plate between primary plate and ground plane that does not touch either of them, is used for further matching and beam width adjustment. The designed antenna works for both DVB-T (174–254 MHz) and DAB-T (174–230 MHz) applications. The antenna is fabricated to verify the simulation results. In the entire band, the return loss is equal or greater than 10 dB with average gain of 8.5 dBi. The paper is organized into the following sections. In section II, the geometry of the SSPA is discussed. In Section 3, the experimental results for the SSPA are presented. Then, in the subsequent sections the equivalent lumped element based circuit model of SSPA and effect of the different

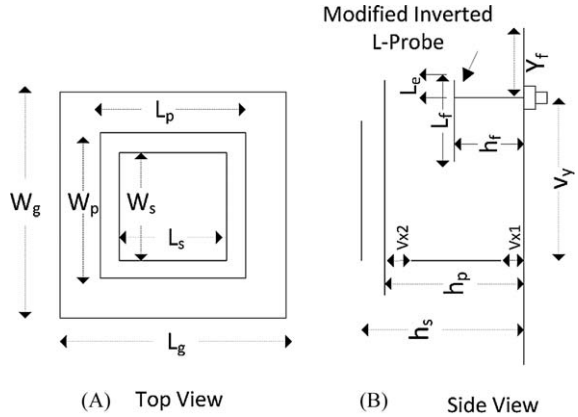

FIGURE 2 Geometry of the SSPA, top, and side view showing different parameters and modified inverted L-probe feed

TABLE 1 Dimensions of SSPA

Type	Length	Width	Height
Ground plane	$L_g = 0.896\lambda_c$	$W_g = 0.753\lambda_c$	$h_g = 0$
Primary plate	$L_p = 0.394\lambda_c$	$W_p = 0.394\lambda_c$	$h_p = 0.1125\lambda_c$
Secondary plate	$L_s = 0.337\lambda_c$	$W_s = 0.337\lambda_c$	$h_s = 0.1899\lambda_c$
Vertical plate	$L_v = 0.2186\lambda_c$	$W_v = 0.111\lambda_c$	$h_v = 0.1125\lambda_c$

geometrical parameters on the performance of the antenna are discussed.

2 | ANTENNA GEOMETRY

Stacked suspended plate antenna in its basic form consist of feeding mechanism, radiating plate, and ground plane. The most important thing in designing the SSPA is the feeding mechanism. The broadband nature of the SSPA completely relies on the feeding structure.[1,22,23] The feeding mechanism should be wideband and matched to 50 Ω as much as possible. Therefore, we designed a novel wideband triangular shaped feeding structure called modified inverted L probe at center frequency of f_c = 202 MHz (λ_c = 1485 mm).[22,23] The geometrical structure of the SSPA, which include front view, top and side view are illustrated in Figures 1 and 2, respectively.

It must be noted that modified inverted L-probe consist of triangular and rectangular plates, where the triangular plate connects the rectangular plate after a gap of L_e = 6 mm ($0.0043\lambda_c$). This gap to be discussed in the latter section plays a vital role in the adjustment of gain and bandwidth of the SSPA. The dimensions of inverted L-probe feed are ($h_f = 0.07166\lambda_c$, $W_f = 0.1433\lambda_c$, $L_f = 0.1075\lambda_c$). This type of L-probe feeding is different than conventional L-type probe which uses rectangular strip without any edge gap. We chose this type of feeding over conventional L-type since it gives better isolation and wider bandwidth. The position of feed point on ground plane is also important[18] and it is not exactly in the center. The position of feed point (X_f, Y_f, Z_f) is

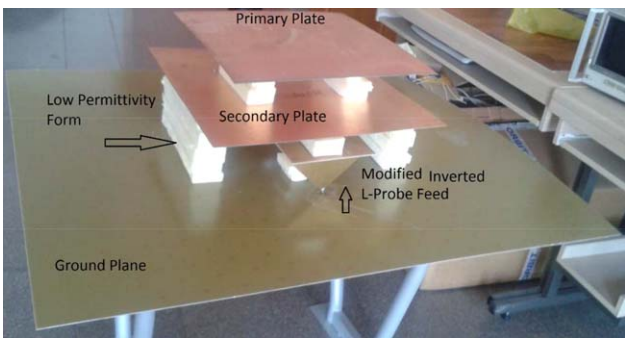

FIGURE 3 Fabricated SSPA, supported by low permittivity foam [Color figure can be viewed at wileyonlinelibrary.com]

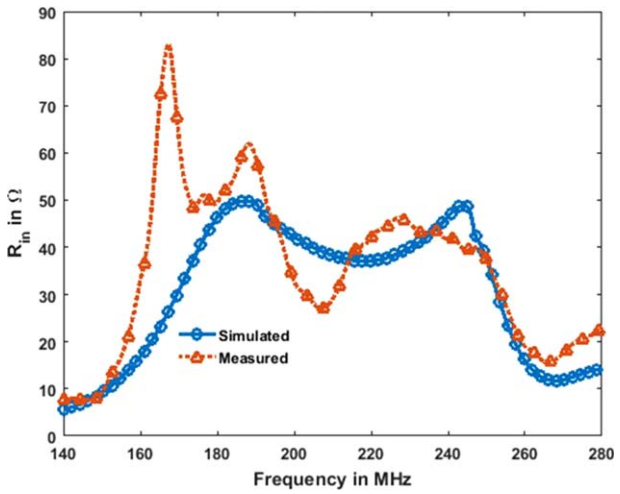

FIGURE 4 Input resistance of the SSPA [Color figure can be viewed at wileyonlinelibrary.com]

(0, L_g/2, $0.197\lambda_c$) selected to get wideband matching. Primary plate is the main radiator, which is excited through electromagnetic coupling by modified inverted L-probe section of SSPA. To get better results for return loss, gain, and bandwidth, a secondary plate is introduced. Further matching and desired beamwidth of the patterns are obtained through the insertion of vertical plate between primary plate and ground plane as shown in Figures 1 and 2, where the small gaps V_{x1} and V_{x2} are equal to 1 mm and 3 mm, respectively. The vertical plate is at $0.493\lambda_c$ from the feed point denoted by V_y. Table 1 summarize rest of the dimensions of the stacked suspended plate antenna. The SSPA is simulated in a commercial full wave solver CST Microwave Studio®.

The antenna is fabricated using 0.1 mm thick copper foil[18] and supported by foam with permittivity of 1.05. The excitation of current or voltage source is done through 50 Ω SMA connector. Figures 2 and 3 shows the fabricated SSPA.

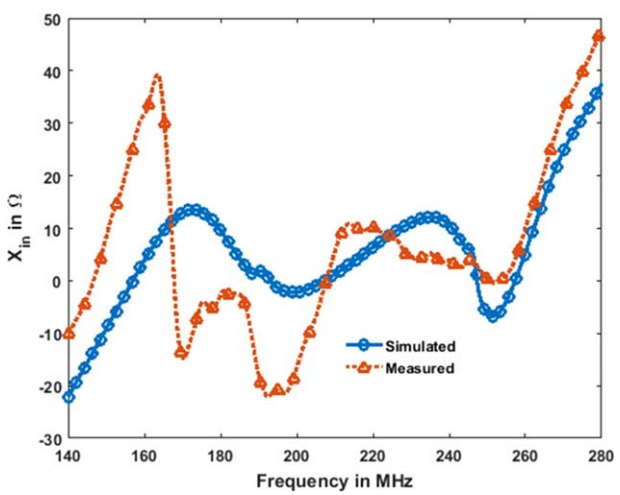

FIGURE 5 Input reactance of the SSPA [Color figure can be viewed at wileyonlinelibrary.com]

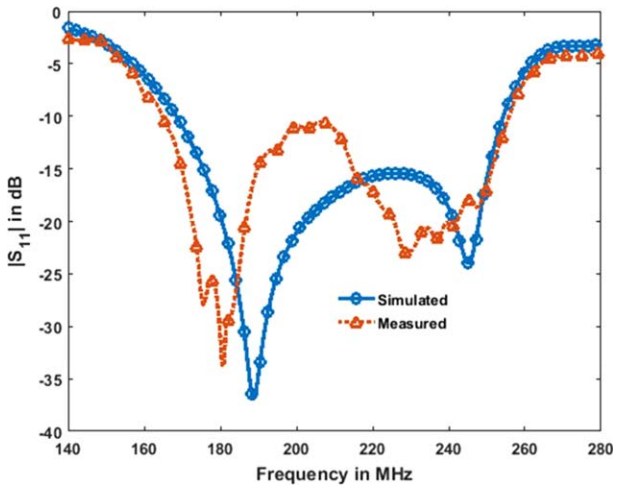

FIGURE 6 Reflection coefficient of the SSPA [Color figure can be viewed at wileyonlinelibrary.com]

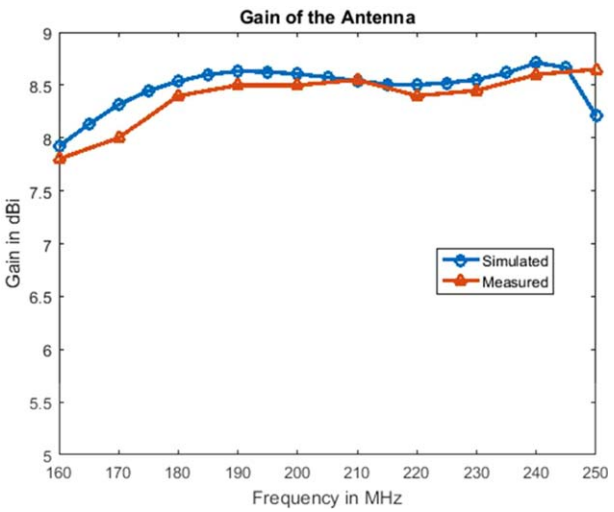

FIGURE 8 Gain of the SSPA [Color figure can be viewed at wileyonlinelibrary.com]

3 | EXPERIMENTAL RESULTS

The performance of the fabricated antenna is tested in several ways by comparing return loss, input impedance, bandwidth, gain, and half power beamwidth with the simulation. In the following sections the experimental results for the input impedance, return loss, gain and radiation patterns of SSPA are reported.

3.1 | Input impedance and return loss

The reflection co-efficient of the SSPA is measured from FieldFox N9912A network analyzer using single port measurement and then, input impedance is extracted to see the resistive and reactive part variation with respect to frequency.

Figures 4 and 5, compare the simulated and measured input resistance and reactance, respectively of the SSPA. Input resistance is varying about 50 Ω in the main bandwidth (174–254 MHz), despite some peaks at certain frequencies in measured resistance. Input reactance is small near the desired band range. However, a large reactance comes from the feeding probe. The measurements are not done in an isolated environment which causes some peaks in measured data. It is observed that a slight movement near the antenna affects the measurements.

Measured and simulated impedances are consistent with each other. Proper selection of dimension can result input resistance of 50 Ω with minimum reactance. For instance, one can determine suitable values for W_f (width of feeding plate) and L_f (length of feeding plate) to cancel the inductance of feeding probe through EM coupling with the primary plate. The heights h_p (height of the primary plate), h_s (height of the secondary plate), and L_e (length of the gap, after which the triangular sheet connects rectangular sheet) must be determined properly to get input impedance close to 50 Ω.

The reflection coefficient, when the SMA connector of 50 Ω is matched with the input impedance of SSPA, is

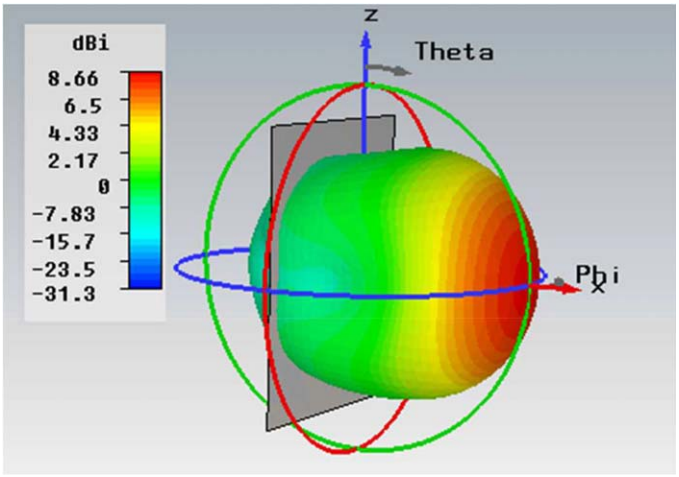

FIGURE 7 3D radiation pattern of the SSPA in CST MWS® at 200 MHz [Color figure can be viewed at wileyonlinelibrary.com]

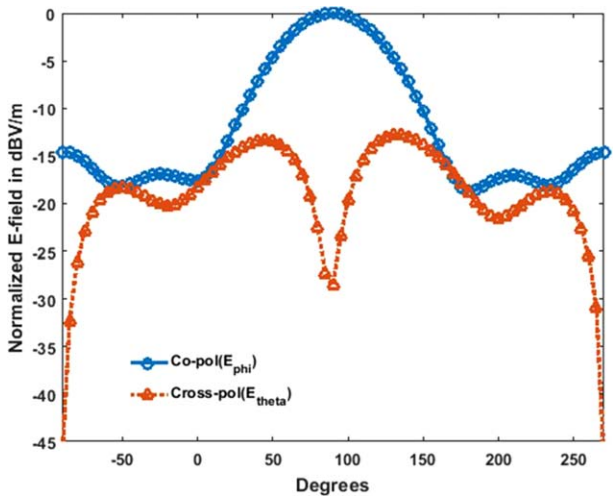

FIGURE 9 Co-polarized and crosspolarized *E*-field patterns in the *E* plane [Color figure can be viewed at wileyonlinelibrary.com]

shown in Figure 6. Both curves show that the antenna has a return loss above 10 dB in the bandwidth of operation. The antenna has fractional impedance bandwidth of about 42%, where the return loss is above 10 dB. At the center frequency, the measured return loss is about 10 dB while in simulation results it is about 17 dB. However, the simulation results generally agree with the measurement.

3.2 | Gain and radiation patterns

The 3D radiation pattern of the antenna showing main beam direction is found from simulation and plotted in Figure 7. Figure 8 shows maximum gain of the SSPA in the desired frequency band. The antenna gives average gain of about 8.5 dBi in the desired frequency band. The gain of antenna increases marginally with the increasing frequency. A gain of 8.5 dBi is measured at 200 MHz, while in simulation it is

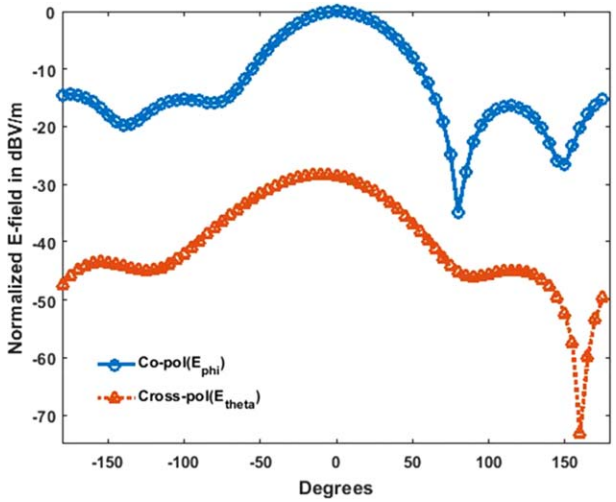

FIGURE 10 Co-polarized and crosspolarized *E*-field patterns in the *H* plane [Color figure can be viewed at wileyonlinelibrary.com]

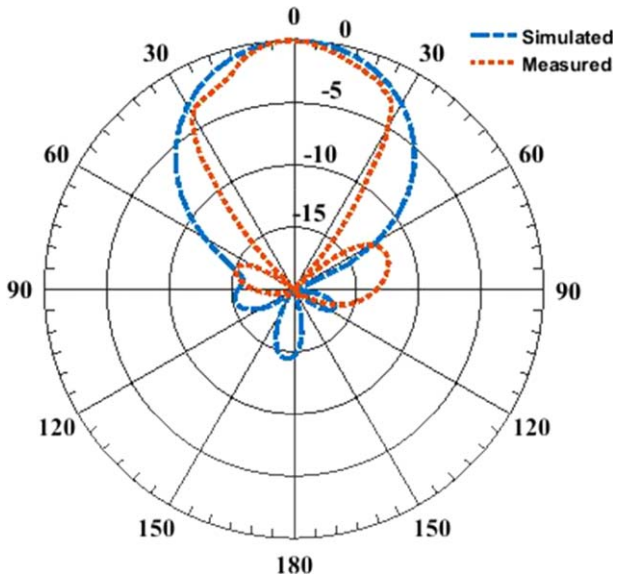

FIGURE 11 Far-field pattern of the SSPA antenna, horizontal pattern at $f = 200$ MHz [Color figure can be viewed at wileyonlinelibrary.com]

8.66 dBi. The measured gain shows that fabricated SSPA performs similar to simulation. As will be seen in the subsequent sections that the desired gain can be obtained by adjusting carefully the height of primary plate, position of vertical plate from the feed position and the edge length.

Another important property of the SSPA is the crosspolarization discrimination (XPD). Its level must be such that both vertical and horizontal fields or vice versa can be distinguished. *E* plane is defined as the plane containing electric field vector and direction of maximum radiation, whereas *H* plane contains magnetic field vector and direction of maximum radiation. For a vertically-polarized antenna, the

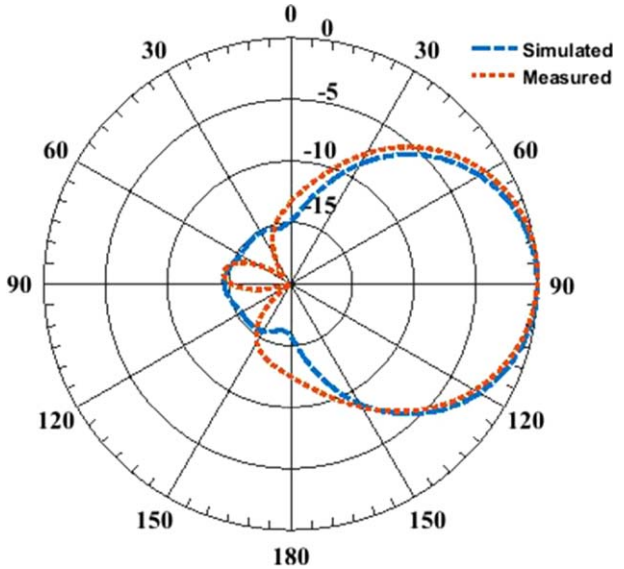

FIGURE 12 Far-field pattern of the SSPA antenna, vertical pattern at $f = 200$ MHz [Color figure can be viewed at wileyonlinelibrary.com]

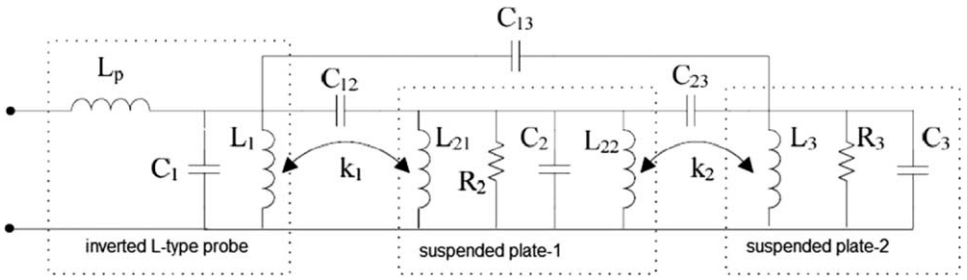

FIGURE 13 Equivalent lumped element circuit model of the SSPA

TABLE 2 Lumped element values

Capacitance	Inductance	Resistance
C_1 = 8.05 pF	L_p = 0.358 pH	R_2 = 26.81 Ω
C_2 = 15.5 pF	L_1 = 17.22 nH	R_3 = 50 Ω
C_3 = 5.4 pF	L_3 = 19.4 nH	
C_{12} = 10 pF	L_{21} = 4.65 nH	
C_{13} = 17.61 pF	L_{22} = 0.221 nH	
C_{23} = 8.147 pF		

E-plane usually coincides with the vertical/elevation plane and *H* plane coincides with the horizontal/azimuthal plane.

The discrimination between co- and crosspolarization can be found from the co-to-cross-pol ratio[1] and the co-to-cross-pol ratio is defined as

$$\text{co-to-cross-pol ratio} = \left(\frac{\text{max. co-pol. rad. level}}{\text{max. cross-pol. rad. level}}\right) \quad (1)$$

For vertically polarized antenna the ratio is given by:

$$\text{co-to-cross-pol ratio} = \left(\frac{\text{max. vert. polarized } |\bar{E}|}{\text{max. hori. polarized } |\bar{E}|}\right) \quad (2)$$

The simulated 3D pattern of the antenna at 200 MHz is shown in Figure 7. In the plot, the green circle shows *E* plane when $\phi = 0°$ while the blue circle shows *H* plane when $\theta = 90°$. The simulated copolarized and crosspolarized *E* fields in *E* and *H* planes are plotted in Figures 9 and 10, respectively. In both planes the co-to-cross-pol ratio must be at least 15 dB within ±20° of the main beam. The plots show that in both planes, the XPD is about 28 dB along the main beam direction. Considering ±20° of the main beam, the antenna gives XPD of 27 dB and 15 dB in *H* and *E*-plane, respectively. The simulated horizontal and vertical radiation patterns are compared with the measurement in Figures 11 and 12, respectively. The measured half power beam width in horizontal plane is 55° while in simulation it is 61°. The measured half power beamwidth in vertical plane is 71° however, in simulation it is 68°. The side lobe level is found to be around −14.4 dB. In general, there is good agreement between simulation and measurement. Therefore, the SSPA is suitable for DVB-T and T-DAB transmission application with stable gain of 8.5 dBi. The beamwidth and side lobe level can be control with the vertical plate position and

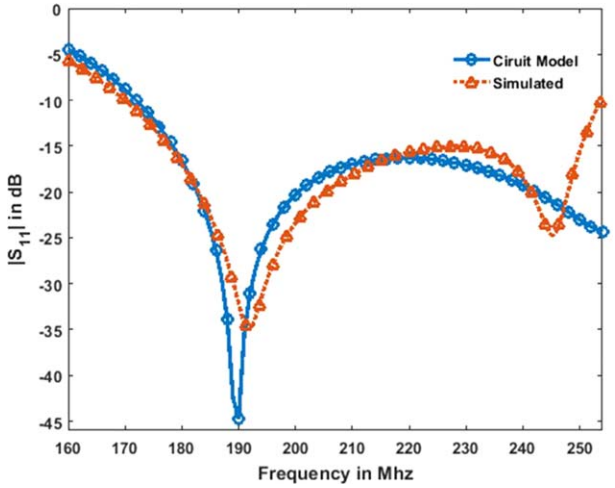

FIGURE 14 Magnitude of S_{11} from the equivalent lumped element circuit model of the SSPA [Color figure can be viewed at wileyonlinelibrary.com]

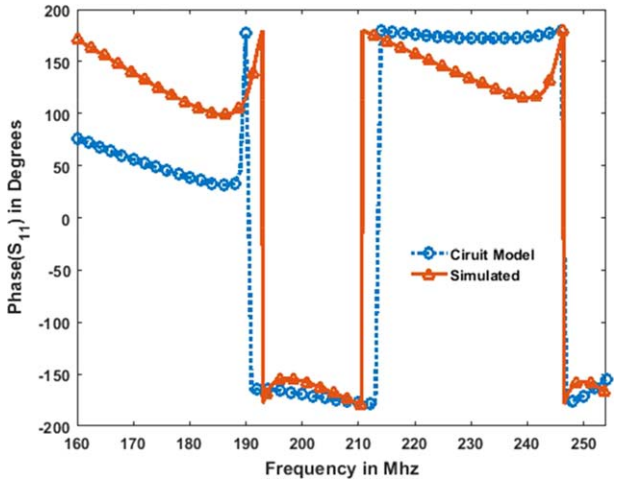

FIGURE 15 Phase of S_{11} from the equivalent lumped element circuit model of the SSPA [Color figure can be viewed at wileyonlinelibrary.com]

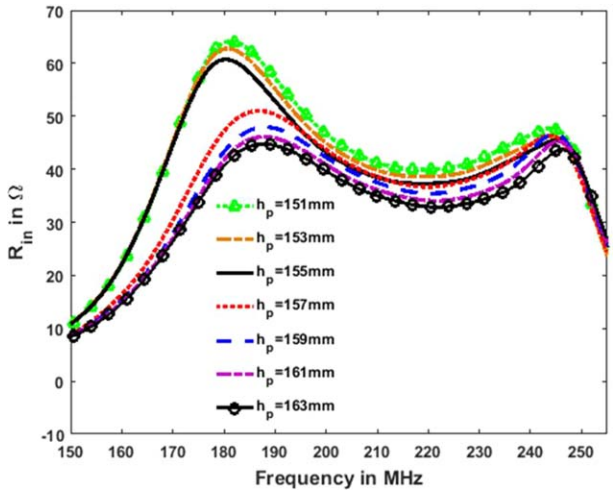

FIGURE 16 Effect of the primary plate height on input resistance of the SSPA [Color figure can be viewed at wileyonlinelibrary.com]

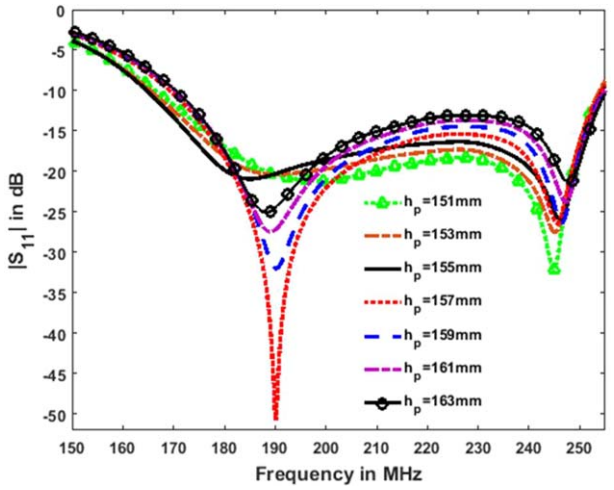

FIGURE 18 Effect of the primary plate height on reflection coefficient of the SSPA [Color figure can be viewed at wileyonlinelibrary.com]

ground plane size, respectively. The side lobe level can be further reduced if we use a ground plane of large size.

4 | EQUIVALENT CIRCUIT MODEL

Figure 13 depicts the equivalent lumped element circuit model of the SSPA. In the model L_p represents the inductance of the L-section modified inverted probe. In the figure, the subscript represents self or mutual reactance. For instance, C_1 and L_1 are the self-capacitance and inductance of rectangular patch of modified inverted L-probe feed, while C_{12} give the mutual capacitance of the rectangular patch of modified inverted L-probe feed and primary plate. The equivalent circuit model is studied via AWR microwave office®. The values of the lumped elements are obtained by studying the structure of the antenna. For instance, the capacitance are calculated by measuring common area of the particular plates and separation between them. These values are further refined in AWR and tabulated in Table 2. The magnitude and phase of the input reflection coefficient are obtained from the circuit model and compared with the simulation in Figures 14 and 15, respectively.

The lumped element circuit model of the SSPA gives reasonable performance in the desired frequency band. It helps in understanding the working of the SSPA.

5 | EFFECT OF THE GEOMETRICAL PARAMETERS ON THE PERFORMANCE OF THE SSPA

In this section, the effect of some geometrical parameters on the characteristics of SSPA such as input impedance, return loss, bandwidth and gain are demonstrated. Such study of geometrical parameters is important and it helps in

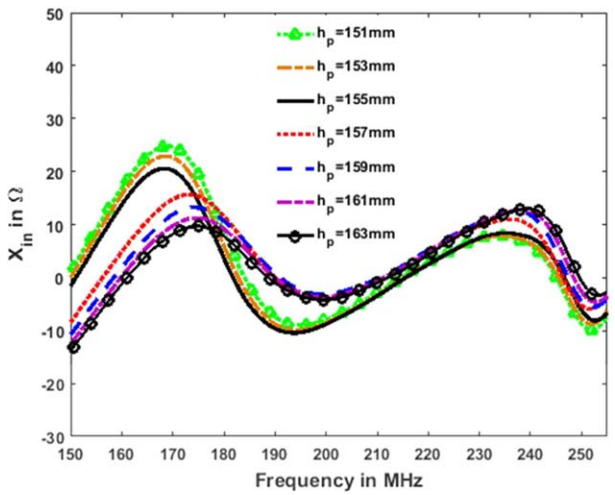

FIGURE 17 Effect of the primary plate height on input reactance of the SSPA [Color figure can be viewed at wileyonlinelibrary.com]

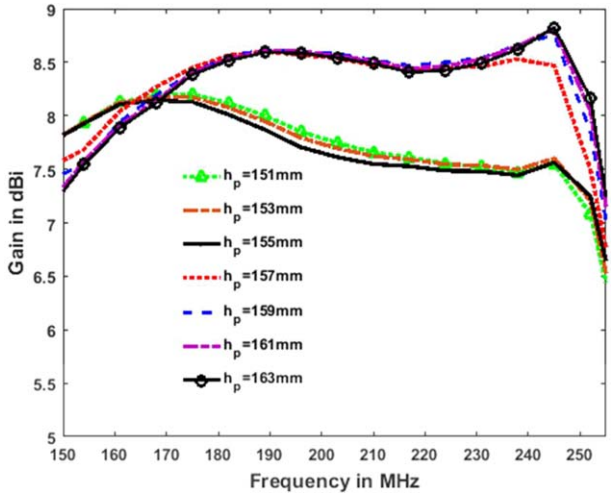

FIGURE 19 Effect of the primary plate height on the gain of the SSPA [Color figure can be viewed at wileyonlinelibrary.com]

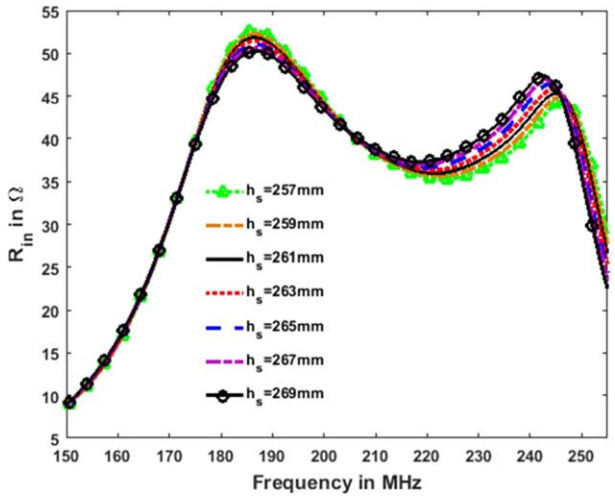

FIGURE 20 Effect of the secondary plate height on input resistance of the SSPA [Color figure can be viewed at wileyonlinelibrary.com]

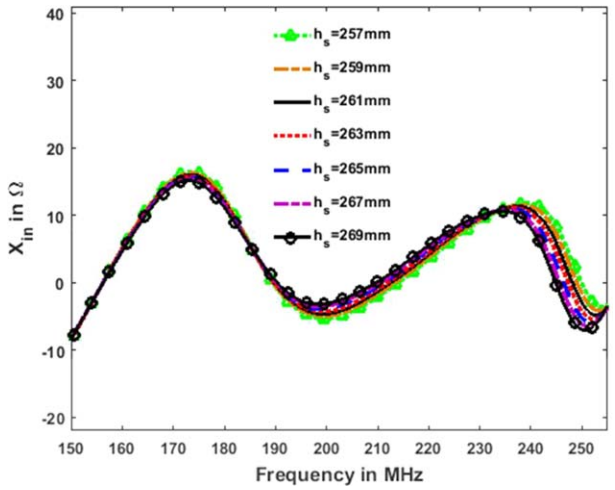

FIGURE 21 Effect of the secondary plate height on the input reactance of the SSPA [Color figure can be viewed at wileyonlinelibrary.com]

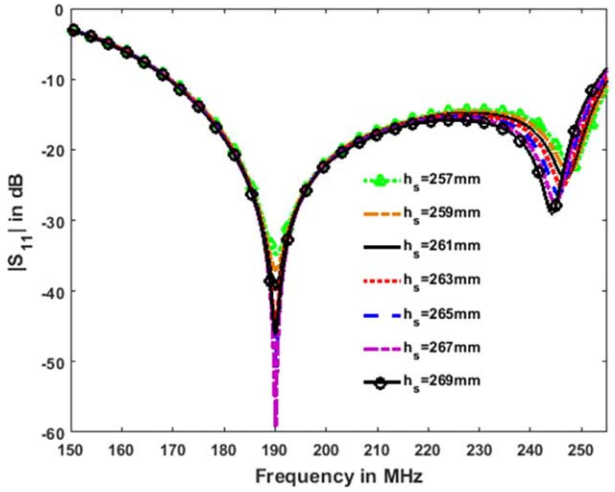

FIGURE 22 Effect of the secondary plate height on reflection coefficient of the SSPA [Color figure can be viewed at wileyonlinelibrary.com]

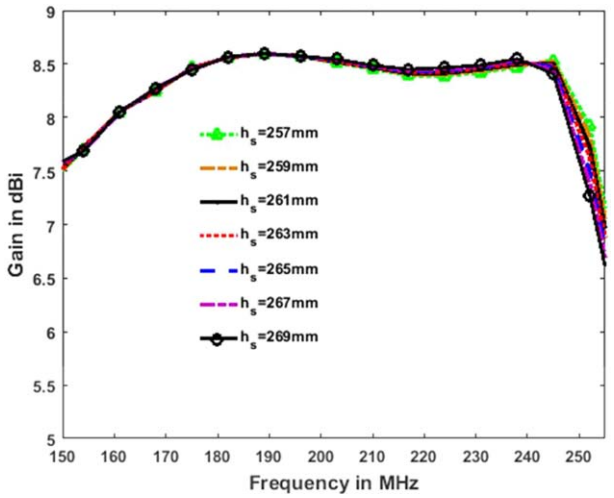

FIGURE 23 Effect of the secondary plate height on gain of the SSPA [Color figure can be viewed at wileyonlinelibrary.com]

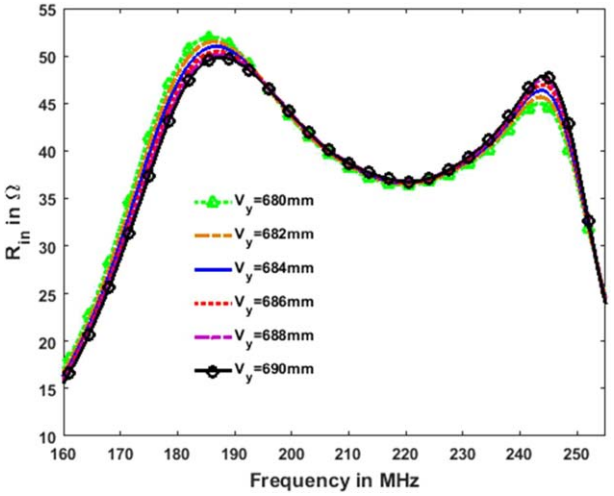

FIGURE 24 Effect of the vertical plate position on input resistance of the SSPA [Color figure can be viewed at wileyonlinelibrary.com]

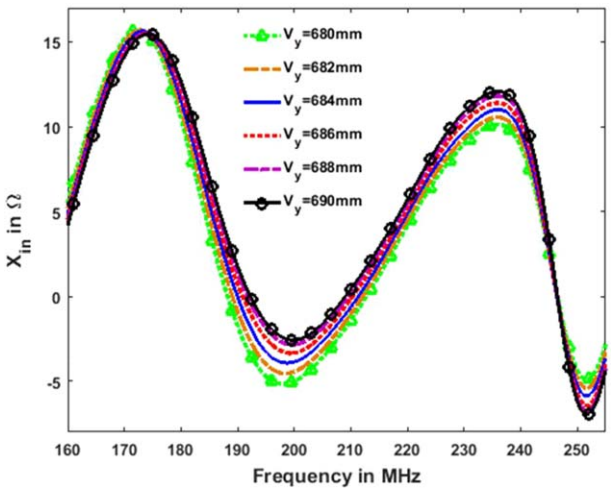

FIGURE 25 Effect of the vertical plate position on input reactance of the SSPA [Color figure can be viewed at wileyonlinelibrary.com]

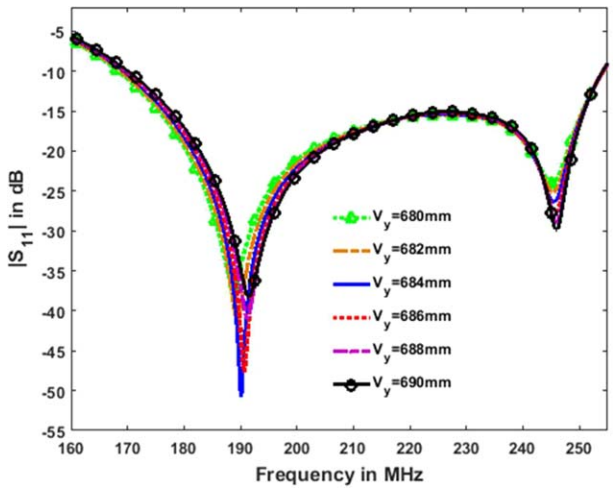

FIGURE 26 Effect of the vertical plate position on reflection coefficient of the SSPA [Color figure can be viewed at wileyonlinelibrary.com]

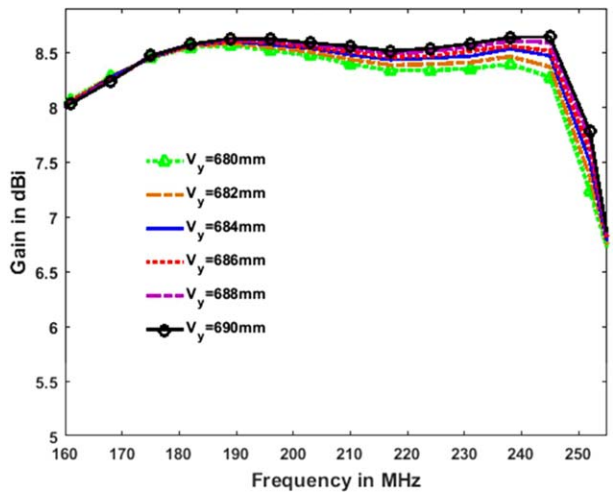

FIGURE 27 Effect of the vertical plate position on gain of the SSPA [Color figure can be viewed at wileyonlinelibrary.com]

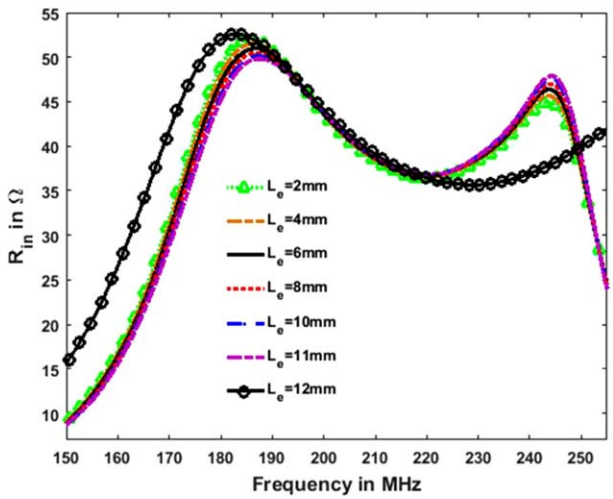

FIGURE 28 Effect of the edge length on input resistance of the SSPA [Color figure can be viewed at wileyonlinelibrary.com]

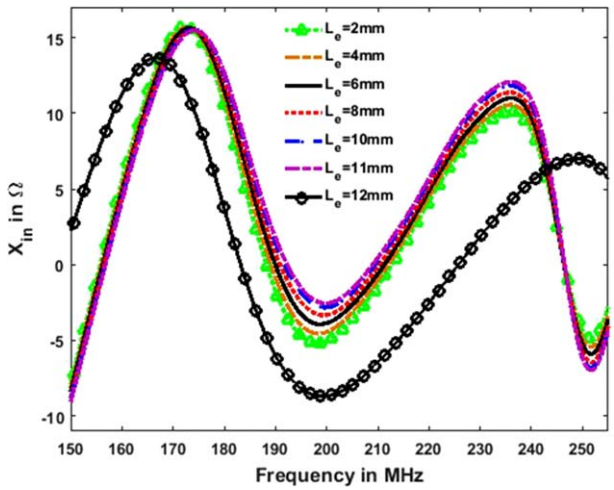

FIGURE 29 Effect of the edge length on input reactance of the SSPA [Color figure can be viewed at wileyonlinelibrary.com]

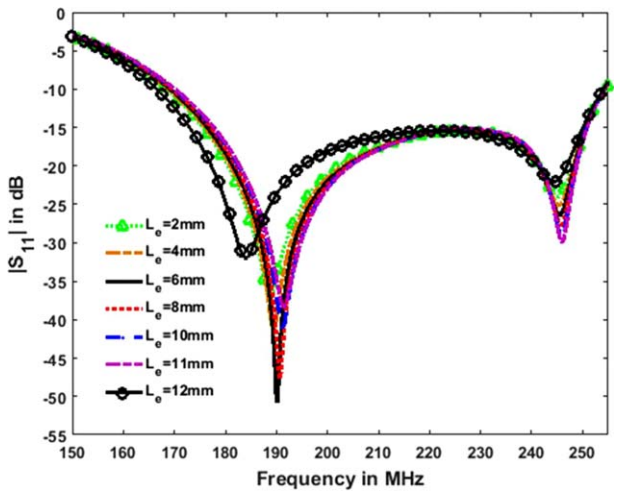

FIGURE 30 Effect of the edge length on reflection coefficient of the SSPA [Color figure can be viewed at wileyonlinelibrary.com]

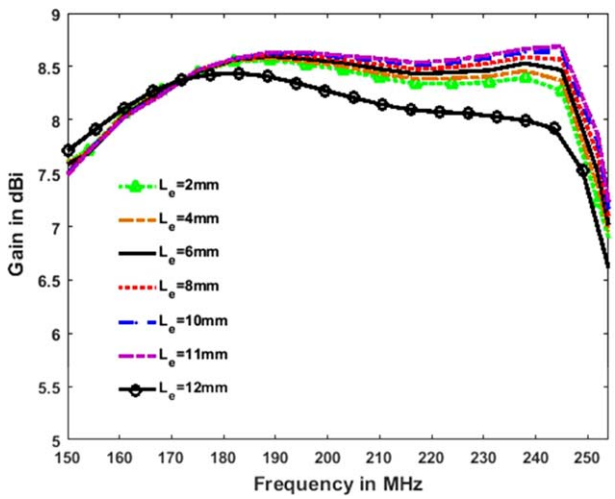

FIGURE 31 Effect of the edge length on gain of the SSPA [Color figure can be viewed at wileyonlinelibrary.com]

understanding the design and operation of the antenna. In addition, it will also help the antenna engineer in designing the antenna for specific properties such as high gain, large bandwidth, and desired half power beamwidth. The effect of geometrical parameters that are studied include h_p (height of the primary plate), h_s (height of the secondary plate), V_y (position of the vertical plate from the feed point), and L_e (length of the edge after which triangular plate connects rectangular plate).

5.1 | The height of primary plate

Primary plate height plays a significant role in matching, gain, and bandwidth enhancement, because there is strong coupling between feeding structure and primary plate. It is varied from 151 to 163 mm with 2 mm step size. Figures 16 and 17 illustrate the effect of primary plate height on the input impedance. Small heights give larger impedance in the lower band. As the height increases the impedance get decreased. At a height of 157 mm, the input resistance is around 35–50 Ω while input reactance stays around −5 to 13 Ω.

Furthermore, Figures 18 and 19 show reflection coefficient and gain of the antenna, respectively. The suitable value for the h_p can be deduce from magnitude of S_{11} and gain. Although height below 157 mm gives slightly wider bandwidth, but it gives low gain as the frequency increases. Similarly, large values for height may give high gain, but it will not be wideband. Large height decreases the coupling between the primary plate and feeding probe, which in turn affects the matching at high frequency. Therefore, the suitable value for the height of primary plate 157 mm as it gives high gain and good matching in the desired frequency bandwidth.

5.2 | The height of secondary plate

The height of the secondary plate (h_s) is varied from 257 to 269 mm. Input resistance, input reactance, return loss, and gain are plotted in Figures 20–23 orderly. It can be seen from the plots that the effect of the height (h_s) of the secondary plate on the impedance, magnitude of S_{11}, and gain can be ignored, despite minimal effect in higher band.

The return loss also remained almost unchanged with secondary plate height. However, at the frequency near 190 MHz the return loss get lowered with h_s variation. Since, in between feeding structure and secondary plate, there is primary plate, so the coupling between them is minimum, which can be the reason for input impedance to remain intact. It must be noted that the secondary plate height variation has minimum effect on the properties of the antenna, however, its presence is important for matching, gain enhancement, and beamwidth adjustment.

5.3 | Position of the vertical plate

Vertical plate is placed at certain distance from modified inverted L-probe feeding element. It is mainly used for half power beamwidth adjustment. However, its position from the origin is varied between 680 and 690 mm to see the effect on the aforementioned properties of the SSPA.

The effect of the vertical plate position on the input resistance, reactance, return loss, and gain are depicted in Figures 24–27, respectively. The figures show that the effect of V_y on the impedance and return loss is minimum, but placing it at a far distance from feed point, increases the gain of antenna that in turn decrease the beamwidth. The best position for the vertical plate is considered as 688 mm. The vertical plate blocks some of the electromagnetic energy to increase the directivity of the SSPA, while decrease beamwidth.

5.4 | Length of the edge

The length of the segment (L_e) after which triangular plate connects rectangular plate is varied from 2 to 12 mm. The modified inverted L-probe cancels the excessive inductance coming from feed probe through electromagnetic coupling with primary plate. In this sense, L_e is important for matching and tuning.

The effect of L_e on SSPA properties such as input resistance, input reactance, reflection coefficient are illustrated in Figures 28–31, respectively. Input resistance and reactance reaches to its maximum if L_e is 0 mm.[18] Increasing its value changes the return loss which ultimately improves the bandwidth of the antenna. Although beyond 11 mm it gives wider bandwidth, but at the same time gain gets decreased. So, a nominal value for L_e is taken as 6 mm with wider bandwidth and acceptable gain in the band of operation.

6 | CONCLUSION

A wideband SSPA antenna is designed for DVB-T and DABT transmission which gives radiation pattern similar to that of dipole antenna. The antenna gives fractional bandwidth of about 42.14% for $S_{11} < -10$ dB and co-to-cross polarization discrimination of about 28 dB in both planes (main beam direction). However, in *H*-plane with ±20° of the main beam XPD of 27 dB is observed while in *E*-plane it is 15 dB. The antenna gives stable average gain of 8.5 dBi in the operating bandwidth. The half power beamwidth of about 55° is achieved in horizontal plane while 71° in vertical plane. Equivalent circuit of the model and effect of the different parameters on the performance of SSPA are presented. The stacked suspended plate antenna is important and may replace the dipole antenna array which requires a mechanism to feed the different elements of the antenna. This study can be applied in future to design antennas at high frequencies.

ORCID

Abdul Ali http://orcid.org/0000-0002-0095-6702

REFERENCES

[1] Chen ZN, Chia MYW. *Broadband Planar Antennas: Design and Applications*. Chichester, England; Hoboken, NJ: John Wiley & Sons; 2006.

[2] Pozar D, Schaubert MD, IEEE Antennas and Propagation Society, (Eds.). *Microstrip Antennas: The Analysis and Design of Microstrip Antennas and Arrays*. New York: Institute of Electrical and Electronics Engineers; 1995.

[3] Ge Y, Esselle KP, Bird TS. A compact E-shaped patch antenna with corrugated wings. *IEEE Trans Antennas Propag.* 2006;54(8):2411–2413.

[4] Chair R, Mak C-L, Lee K-F, Luk K-M, Kishk AA. Miniature wide-band half U-slot and half E-shaped patch antennas. *IEEE Trans Antennas Propag.* 2005;53(8):2645–2652.

[5] Matin MA, Sharif BS, Tsimenidis CC. Probe fed stacked patch antenna for wideband applications. *IEEE Trans Antennas Propag.* 2007;55(8):2385–2388.

[6] Chen ZN, Chia MYW, Lim CL. A stacked suspended plate antenna. *Microw Opt Technol Lett.* 2003;37(5):337–339.

[7] Ning Chen Z, Chia MYW. A feeding scheme for enhancing the impedance bandwidth of a suspended plate antenna. *Microw Opt Technol Lett.* 2003;38(1):21–25.

[8] Chen ZN, Ng JH. Probe-fed center-slotted suspended plate antennas with resistive and capacitive loadings. *Microw Opt Technol Lett.* 2005;45(4):355–360.

[9] Ciydem M, Koc S. High isolation dual-polarized broadband antenna for base stations. *Microw Opt Technol Lett.* 2015;57(3):603–607.

[10] Wu Hu J, Yin WY, Lian R. Broadband circularly polarized antennas with center-slot-feeding. *Microw Opt Technol Lett.* 2015;57(12):2793–2797.

[11] Chen ZN, Chia MYW. A novel center-slot-fed suspended plate antenna. *IEEE Trans Antennas Propag.* 2003;51(6):1407–1410.

[12] Chen ZN, Yan Wah Chia M. Experimental study on radiation performance of probe-fed suspended plate antennas. *IEEE Trans Antennas Propag.* 2003;51(8):1964–1971.

[13] Chen ZN. Suspended plate antennas with shorting strips and slots. *IEEE Trans Antennas Propag.* 2004;52(10):2525–2531.

[14] Huang J, Hussein ZA, Petros A. A VHF microstrip antenna with wide-bandwidth and dual-polarization for sea ice thickness measurement. *IEEE Trans Antennas Propag.* 2007;55(10):2718–2722.

[15] Nasimuddin XQ, Chen ZN. A wideband circularly polarized stacked slotted microstrip patch antenna. *IEEE Antennas Propag Mag.* 2013;55(6):84–99.

[16] Wong H, Lau KL, Luk KM. Design of dual-polarized L-probe patch antenna arrays with high isolation. *IEEE Trans Antennas Propag.* 2004;52(1):45–52.

[17] Chen ZN, Chia MYW. Broadband suspended plate antennas fed by double L-shaped strips. *IEEE Trans Antennas Propag.* 2004;52(9):2496–2500.

[18] Wang Z, Fang S, Fu S. Wideband dual-layer patch antenna fed by a modified L-strip. *J Microw Optoelectron Electromagn Appl.* 2010;9(2):89–99.

[19] Zhi Ning C. Broadband suspended plate antenna with concaved center portion. *IEEE Trans Antennas Propag.* 2005;53(4):1550–1551.

[20] Toh W, Chen Z. On a broadband elevated suspended-plate antenna with consistent gain. *IEEE Antennas Propag Mag.* 2008;50(2):95–105.

[21] Low XN, Chen ZN, Toh WK. Ultrawideband suspended plate antenna with enhanced impedance and radiation performance. *IEEE Trans Antennas Propag.* 2008;56(8):2490–2495.

[22] Ali A. Analysis and design of broadcast tower antenna systems. Master's thesis, Bilkent University; 2014, Ankara, Turkey. http://hdl.handle.net/11693/18319

[23] Ali A, Ciydem M, Altintas A, Koc S. DVB-T and DAB-T transmitter antenna design by using stacked suspended plates. In Proc. of 7th Congress URSI-Turkey; 2014:1–4.

How to cite this article: Ali A, Ciydem M, Altintas A, Koc S. VHF suspended plate transmitter antenna design for DVB-T and DAB-T. *Microw Opt Technol Lett*. 2018;60:1536–1546. https://doi.org/10.1002/mop.31196

Received: 12 October 2017

DOI: 10.1002/mop.31204

Design of a compact dual-band monopole antenna using a top-loaded octagon patch and perforated shorting pin

Jae Sung Park | **Hak Keun Choi**

Department of Electronic Engineering, Dankook University, Gyeonggi-do, Korea

Correspondence
Hak Keun Choi, Department of Electronic Engineering, Dankook University, Gyeonggi-do, Korea.
Email: hkchoi@dankook.ac.kr

Funding information
Dankook University

Abstract

In this article, an antenna operated in the dual band (824-894 and 1750–2800 MHz) is proposed, and its performance is verified. The proposed antenna is structured with a monopole antenna of a reversed crossing trapezoidal type,